22 JANUARY 2007
Volume 90 Number 4

APPLIED PHYSICS LETTERS

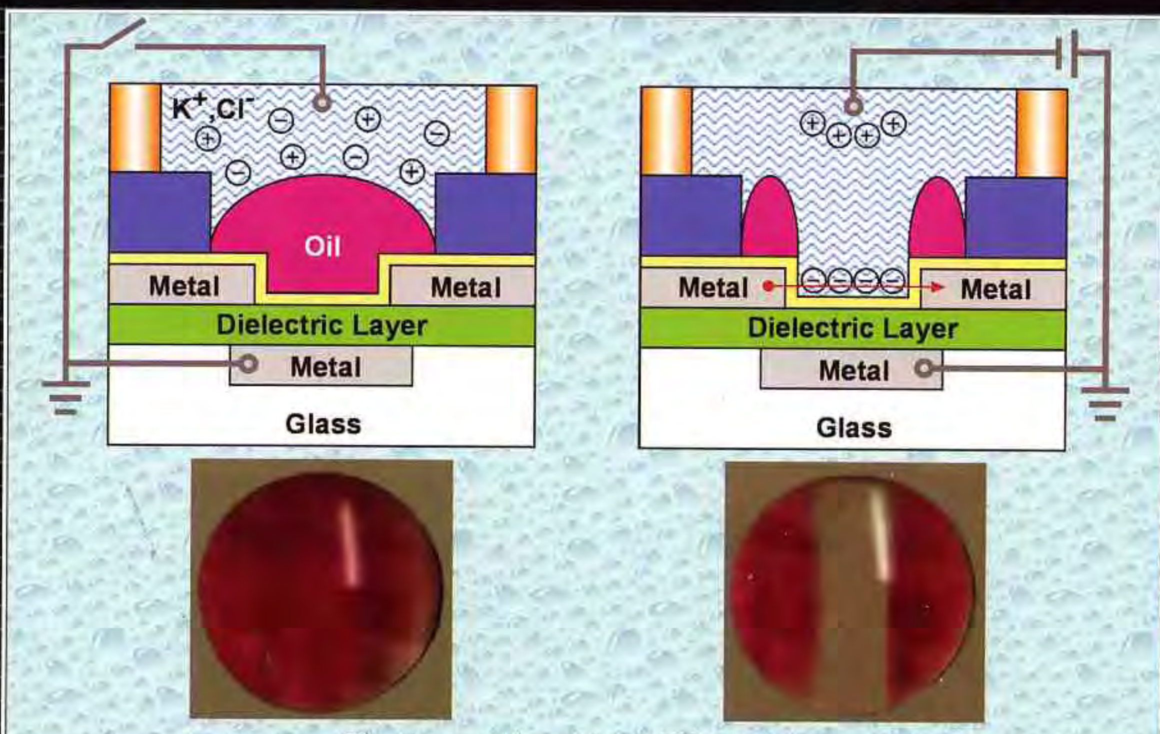

Electrowetting Liquid Transistor

0003-6951(20070122)90:4;1-7

AMERICAN INSTITUTE OF PHYSICS

Liquid-state field-effect transistors using electrowetting

D. Y. Kim and A. J. Steckl[a)]
Nanoelectronics Laboratory, University of Cincinnati, Cincinnati, Ohio 45221-0030

(Received 9 October 2006; accepted 14 November 2006; published online 23 January 2007)

The authors report the demonstration of transistor action in the liquid state. The control of current flow in a liquid field-effect transistor (LiquiFET) was achieved by electrowetting between competitive insulating/conducting fluids. The LiquiFET structure included dielectric/hydrophobic layers, source/drain regions, a gate electrode, and hydrophilic/hydrophobic grids to contain the liquids. For a 400 μm long channel, turn-on occurs at 2.5–3 V drain voltage. On/off current ratios $>$10 000:1 were measured. Linear gate voltage control over drain current was obtained with a transconductance up to 40 nS. A calculated channel mobility of $\sim$1 $cm^2/V\,s$ indicates that electronic charge transport dominates transistor operation. © *2007 American Institute of Physics*.
[DOI: 10.1063/1.2435508]

Interest in microfluidic science and devices is growing rapidly due to important applications ranging from biotechnology[1] to flat panel displays.[2] An important enabling technology in microfluidics is based on the electrowetting effect,[3,4] which controls the contact angle of a liquid on a hydrophobic surface through the application of an electric field. Manipulation of a liquid droplet is readily achieved[5] by sequential actuation of adjacent control electrodes. Many operations can be performed through external control,[6,7] such as droplet dispensing, transport, splitting, and mixing. This has led to increasingly sophisticated applications for *laboratory-on-chip*[8,9] devices.

One of the limitations of microfluidic devices is that the information contained in the fluid has to be converted into an electronic form in order to interact with our pervasive digital electronic world. This conversion typically is performed through either direct optical sensing (using a video camera or a detector) or combined with optical excitation of fluorescent dyes. This approach is cumbersome, limited in information processing, and expensive. Here we report on liquid-state field-effect transistors (LiquiFETs), an approach that promises to integrate intimately microfluidics and microelectronics. Recently, liquid electronic devices have focused on ion transport in nanometer-scale liquid channels. For example, Stein *et al.* have investigated[10] the effect of surface charge nanofluidic channels and Karnik *et al.* have reported[11] electrostatic control of charged particles in nanofluidic channels. The main objective of the work reported here is the design and fabrication of an electrowetting-based LiquiFET, which is very similar in concept to conventional semiconductor FETs but operates in the liquid state and thus can directly convert charge-related information from the liquid state into conventional electronic signals.

The basic LiquiFET operation and device structure are illustrated in Fig. 1. Control of current flow in the LiquiFET is obtained by controlling the presence in the channel of one of two fluids: a conducting fluid (aqueous electrolyte) or an insulating fluid (nonpolar oil). Figure 1 shows the principle of the electrowetting-based LiquiFET. Fluid location in the channel region is determined by the electric field applied to the gate through the competitive electrowetting effect. We used a water droplet with KCl as the conducting medium and an oil film (with a nonpolar dye for visualization purposes) for the electrical switching.

Figures 1(a) and 1(b) show the cross-section (a-a' section) schematics of the LiquiFET under off (zero gate bias) and on (negative gate bias) conditions, respectively. The similarity to the cross section of a conventional solid state metal-oxide-semiconductor field-effect transistor (MOSFET) is clear. The device structure consists of the glass substrate, a dielectric-covered transparent ground electrode, source and drain metal contacts, a hydrophobic insulator layer (amorphous fluoropolymer), a hydrophobic/hydrophilic grid, the two fluids (electrolyte/oil), and the top gate electrode (Au wire). For zero gate bias, the low surface tension oil preferentially covers the low surface energy hydrophobic insulator, forming a thin film that excludes the high surface tension polar electrolyte solution. The circular active device area [Fig. 1(c)] is defined by the hydrophilic grid, which confines

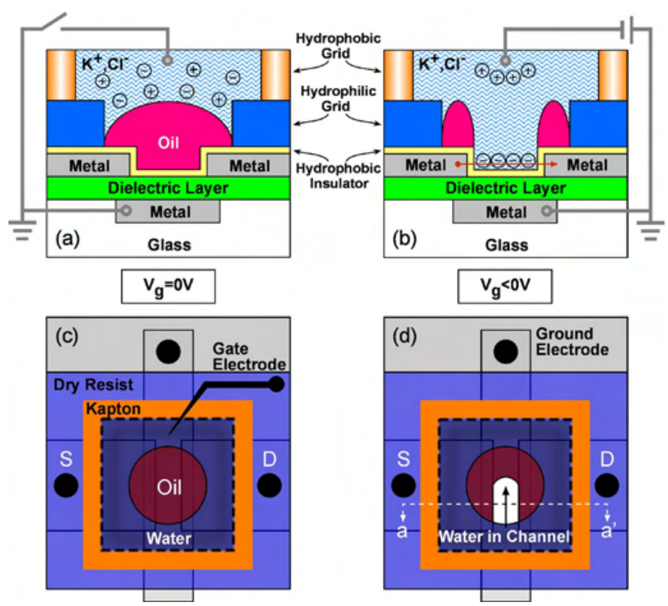

FIG. 1. (Color online) Schematic diagrams of LiquiFET structure: (a) cross section in off state, (b) cross section (a-a' section) in on state, (c) top view in off state, and (d) top view in on state [the a-a' section corresponding to (b) is shown as a dashed line].

[a)]Author to whom correspondence should be addressed; electronic mail: a.steckl@uc.edu

the oil by strongly attracting water molecules. When a negative bias is applied to the gate, the resulting field across the hydrophobic insulator effectively increases its surface energy and reduces its hydrophobicity, attracting the polar water molecules and electrolyte anions to the insulator surface. The water increasingly displaces the oil layer with increasing bias and forces the displaced oil to the side regions of the structure, as shown in Fig. 1(b). The top view in Fig. 1(d) includes a cross-section line (a-a') which shows its relationship to the cross-section view of Fig. 1(b). The electrolyte makes an initial contact to the hydrophobic surface at one of the ends of the channel [Fig. 1(d)] because the oil thickness at the outer edges of the channel is lower than in the center of the channel. This is similar to the oil thickness profile depicted qualitatively *along* the channel in the schematic diagram in Fig. 1(a). In the process, the presence of the electrolyte in the channel region between source and drain opens the channel for current conduction. When the gate bias is removed the oil returns to its original position [Fig. 1(c)] due to the capillary force acting to minimize the energy of the system.

For the results reported here, the LiquiFET channel has a length of 400 μm (defined by the spacing between source and drain electrodes) and a width of 1400 μm (equal to the oil drop diameter). The hydrophobic insulator and the underlying insulator layers are typically 40 and 300 nm thick, respectively. The ground, source, and drain electrodes consist of 200 nm indium tin oxide (ITO) layers. A 30 μm high hydrophilic grid uses patterned photoresist to confine an 80 nL oil droplet. Finally, a 3×3 mm^2 hydrophobic grid is formed using polyimide to confine a 30 μL water droplet.

The ITO ground electrode was patterned by lift-off photolithography on the starting glass substrate. The ITO layer was deposited by sputtering from a 90%/10% In_2O_3/SnO_2 target followed by rapid thermal anneal (RTA) at 450 °C for 3 min in nitrogen. The 200 nm ITO layer had a sheet resistance of 30 $\Omega/\square$ after RTA. A combination of Si_3N_4 and spin-on-glass (SOG) formed the dielectric layer. Si_3N_4 was sputtered in Ar and annealed at 500 °C for 1 h in nitrogen ambient. Next, SOG (IC1-200, Futurrex Inc.) was spin coated and annealed. The thickness of the Si_3N_4 and SOG layers were typically 200 and ~100–150 nm, respectively.

The source and drain electrodes consisted of 200 nm of sputtered ITO. The ITO deposition and patterning were the same as those used for the ITO ground electrode. Amorphous fluoropolymer was used for the hydrophobic insulator in the electrowetting structure. A 1% fluoropolymer solution in fluorosolvent was spin coated to form a 40 nm film. Next, the fluoropolymer film was dried for ~4 h at room temperature in air, producing a surface energy of 16 dyn/cm. A subsequent anneal at 180 °C optimizes the adhesion and reduces the surface energy to 14 dyn/cm.

The hydrophilic grid was formed using dry photoresist (MM115i, Think & Tinker, Ltd.). The dry resist has a thickness of 30 μm and a surface energy[12] of ~40 dyn/cm. The dry film was attached to the sample and laminated using a dry film laminator. The negative dry film was exposed to define an active device region. Then the film was developed using 1 wt % sodium carbonate monohydrate ($Na_2CO_3 \cdot H_2O$).

The final element of the LiquiFET device structure is the hydrophobic grid necessary to contain the water droplet. A polyimide-based tape (Dupont Kapton) was used for this purpose. To operate the LiquiFET, a 30 μL droplet of 0.05M KCl was placed on the hydrophobic surface. Then 80 nL of dodecane ($C_{12}H_{26}$) (Acros) with a nonpolar red dye (Keystone Aniline Corp.) was injected using a microsyringe. The red dye was purified by column chromatography to separate out polar impurities incorporated into the dye. These polar impurities hinder oil movement and result in higher voltages for electrowetting to occur. Due to the different surface energy between them, the dodecane (25 dyn/cm) oil naturally locates itself between the hydrophobic surface (fluoropolymer, 14 dyn/cm) and the electrolyte (water,[13] 72 dyn/cm).

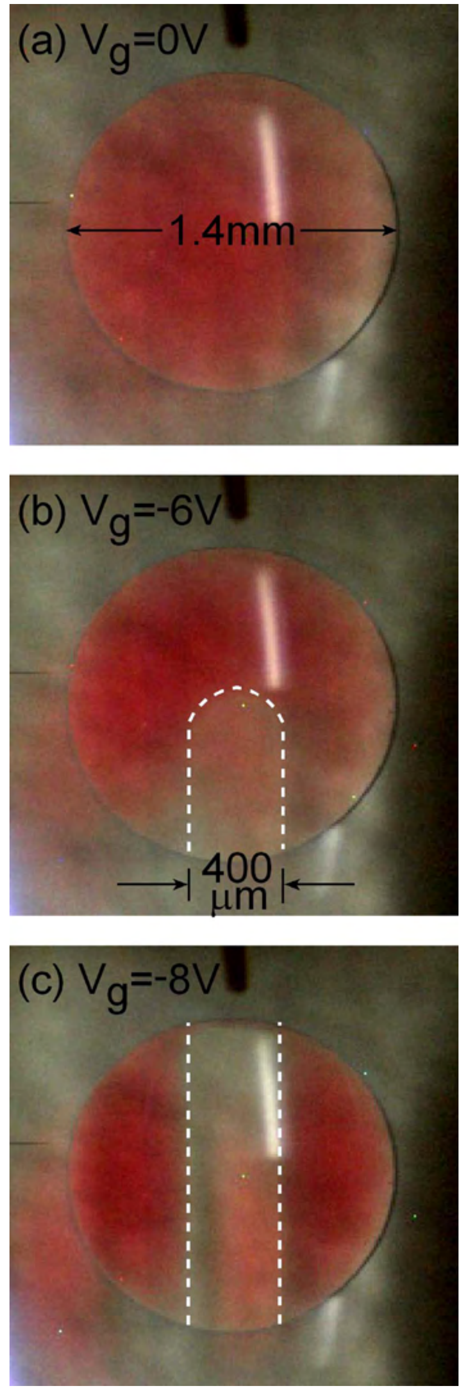

FIG. 2. (Color online) Photographs of LiquiFET showing the effect of gate voltage on fluid location in the channel: (a) 0, (b) −6, and (c) −8 V.

The LiquiFET in operation is seen in Fig. 2, where photographs show displacement of the oil droplet in the channel

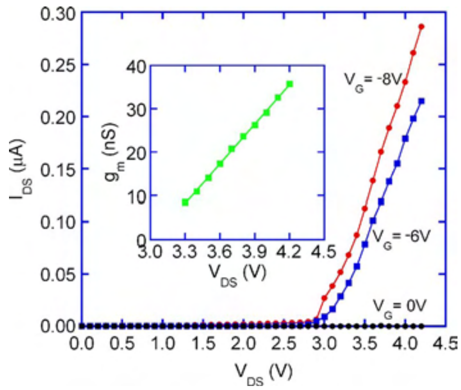

FIG. 3. (Color online) LiquiFET output characteristics: drain current vs drain voltage at different values of gate voltage. Insert: transconductance characteristics.

region of an actual device. At V_G=0 V, there is no electrowetting and the oil layer extends to contact the entire hydrophobic surface in the channel region [see Fig. 2(a)]. In this case, the transistor is in the electrically off state, with the source to drain channel closed to charge transport. As the gate bias is increased, electrowetting starts and the electrolyte is increasingly attracted to the hydrophobic surface, replacing the oil layer. The anions present on (and close to) the fluoropolymer surface effectively form an electrical channel similar to that in a MOSFET. Once the channel is formed, electrons can flow from source to drain through this negative ion channel, establishing the LiquiFET drain current. At V_G =−6 V, approximately half of the channel is active [see Fig. 2(b)]. At a slightly higher voltage of −8 V, the channel is completely open [see Fig. 2(c)]. The white dashed lines were added to more clearly delineate the region from which the oil is displaced and replaced with electrolyte. The reddish tint still visible in the active channel region is due to reflection from other regions and not to oil still present in the channel.

Typical electrical characteristics of the LiquiFET are shown in Fig. 3. The measured source-drain current (I_{DS}) versus drain voltage (V_{DS}) is shown at several values of gate bias. In the absence of gate bias, I_{DS} is negligible. When the gate bias is sufficient to open the channel, significant current flow is obtained. The LiquiFET drain turn-on voltage is 2.8–3.0 V, depending somewhat on gate voltage. The drain current in the off state (V_G=0 V) is below 10^{-11} A and it increases to the 10^{-7} A range in the on state ($V_G > -3$ V). This represents an on/off ratio of $\sim 10^4$:1. The LiquiFET transconductance (g_m) was calculated from I_{DS} vs V_G characteristics. The values of g_m shown in the insert of Fig. 3 vary linearly with V_{DS}. A value of ~30 nS is obtained at V_{DS}=4.2 V. Using the transconductance values and the approximate channel capacitance, we have calculated an effective channel mobility of $\sim 1\ cm^2/V\ s$. This indicates that charge transport in the LiquiFET is predominantly electronic, as ionic mobility is much lower (10^{-4}–$10^{-3}\ cm^2/V\ s$).

The I_{DS} vs V_{DS} characteristics obtained for the LiquiFET depart from those of the conventional semiconductor-based MOSFET in several aspects: the presence of the drain turn-on voltage, low drain current, and absence of drain current saturation. The LiquiFET drain turn-on voltage reflects the charge injection mechanisms into the channel, which have not yet been fully characterized. Among the factors that may contribute to the turn-on voltage are the effective Schottky barrier between the source electrode (ITO) and the channel region, and the tunneling efficiency through the hydrophobic insulator layer. These initial LiquiFET devices did not employ optimized dielectric layers and experienced premature dielectric breakdown. This limited the range of the drain voltage which could be applied and possibly obscured the drain current saturation effect.

In summary, we have reported the operation of MOSFET-like transistors operated in the liquid state and which are controlled by an electrowetting process. The LiquiFET transistor current-voltage characteristics exhibit similarities and differences from those of conventional semiconductor MOSFETs. The LiquiFET may open the door to higher levels of integration (and performance) of fluidic and electronic devices.

This work was partially supported by a grant from the National Science Foundation (ECS-0439074). The authors would like to acknowledge many useful technical discussions with D. Han and J. C. Heikenfeld and the support and encouragement of R. Khosla.

[1] *Microfluidic Techniques*, Methods in Molecular Biology Vol. 321, edited by S. Minteer (Humana, Totowa, NJ, 2006).
[2] J. C. Heikenfeld and A. J. Steckl, Inf. Disp., 26 (2004).
[3] T. B. Jones, J. Micromech. Microeng. **15**, 1184 (2005).
[4] F. Mugele and J. C. Baret, J. Phys.: Condens. Matter **17**, R705 (2005).
[5] M. G. Pollack, R. B. Fair, and A. D. Shenderov, Appl. Phys. Lett. **77**, 1725 (2000).
[6] M. Washizu, IEEE Trans. Ind. Appl. **34**, 732 (1998).
[7] S. K. Cho, H. J. Moon, and C. J. Kim, J. Microelectromech. Syst. **12**, 70 (2003).
[8] J. Y. Yoon and R. L. Garrell, Anal. Chem. **75**, 5097 (2003).
[9] V. Srinivasan, V. K. Pamula, and R. B. Fair, Anal. Chim. Acta **507**, 145 (2004).
[10] D. Stein, M. Kruithof, and C. Dekker, Phys. Rev. Lett. **93**, 035901 (2004).
[11] R. Karnik, R. Fan, M. Yue, D. Li, P. Yang, and A. Majumdar, Nano Lett. **5**, 943 (2005).
[12] J. C. Heikenfeld and A. J. Steckl, Appl. Phys. Lett. **86**, 011105 (2005).
[13] A. W. Adamson and A. P. Gast, *Physical Chemistry of Surfaces* (Wiley, New York, 1997), p. 36.